

# Pakistan Veterinary Journal

ISSN: 0253-8318 (PRINT), 2074-7764 (ONLINE) DOI: 10.29261/pakvetj/2025.278

# RESEARCH ARTICLE

# Comparison of Classical and Atypical Forms of Ovine Pulmonary Adenocarcinomas Using Immunohistochemical and Molecular Techniques

Emin Karakurt<sup>!,\*</sup>, Nüvit Coşkun<sup>2</sup>, Ömer Faruk Keleş<sup>3</sup>, Enver Beytut<sup>1</sup>, Turan Yaman<sup>3</sup>, Ayfer Yıldız Uysal<sup>1</sup>, Selda Güneş<sup>4</sup>, Hacı Ahmet Çiçek<sup>5</sup>

<sup>1</sup>Department of Pathology, Faculty of Veterinary Medicine, Kafkas University, Kars, Türkiye, 36100; <sup>2</sup>Department of Virology, Faculty of Veterinary Medicine, Kafkas University, Kars, Türkiye, 36100; <sup>3</sup>Department of Pathology, Faculty of Veterinary Medicine, Van Yuzuncu Yil University, Van, Türkiye, 65080; <sup>4</sup>Institute of Health Sciences, Kafkas University, Kars, Türkiye, 36100; <sup>5</sup>Institute of Health Sciences, Van Yuzuncu Yil University, Van, Türkiye, 65080 \*Corresponding author: mehmeteminkarakurt@hotmail.com

#### ARTICLE HISTORY (25-683)

#### Received: July 13, 2025 Revised: September 21, 2025 Accepted: October 04, 2025 Published online: October 16, 2025

#### Key words:

Immunohistochemistry Jaagsiekte Sheep Retrovirus Ovine Pulmonary Adenocarcinomas RT-PCR

#### ABSTRACT

This study aimed to evaluate the classical and atypical forms of ovine pulmonary adenocarcinomas (OPA) by immunohistochemical and molecular methods. OPA forms were compared among themselves in terms of proliferating cell nuclear antigen (PCNA), p53 tumour suppressor gene, carcinoembryonic antigen (CEA) and vascular endothelial growth factor-A (VEGF-A) expressions. Avidin-biotin-peroxidase method was used for immunohistochemistry. Half of the cases were classified as classical form and other six were determined to be atypical form. All of the OPA forms had positive reactions for PCNA, p53, CEA and VEGF-A immunoreactivity. However, immunohistochemical and statistical analyses indicated no significant difference between the classical and atypical forms of OPA. In addition, Jaagsiekte sheep retrovirus nucleic acid detection was investigated using reverse transcription polymerase chain reaction (RT-PCR). Nucleic acids from paraffinated tissue blocks were isolated using a phenol/chloroform based method. Reverse transcription and polymerase chain reaction was performed using 2X One-step RT-PCR kit (Hibrigen, Türkiye, Catalogue Number: MG-OSPM-01). Five of the paraffin-embedded tissue samples (5/12) tested positive. Positive amplicons were sequenced and sequence data revealed that all isolates were type 2 exogenous Jaagsiekte sheep retrovirus (exJSRV), and positive samples contained minor amino acid changes among themselves. In conclusion, immunohistochemical parameters revealed the absence of significant difference between atypical and classical OPAs in terms of cancer dynamics, such as proliferation index, metastasis, angiogenesis capacity, and escape from apoptosis, and molecular methods also supported these findings.

**To Cite This Article:** Karakurt E, Coşkun N, Keleş ÖF, Beytut E, Yaman T, Yıldız Uysal A, Güneş S, Çiçek HA, 2025. Comparison of classical and atypical forms of ovine pulmonary adenocarcinomas using immunohistochemical andmolecular techniques. Pak Vet J. <a href="http://dx.doi.org/10.29261/pakvetj/2025.278">http://dx.doi.org/10.29261/pakvetj/2025.278</a>

### INTRODUCTION

Retroviruses constitute a multifaceted category of enveloped, double-stranded RNA viruses distinguished by their capacity to introduce their genetic material into the genome of the host organism, affecting a multitude of cellular processes and potentially inducing various pathologies (Hodor et al., 2024). Retroviruses cause multiple diseases in sheep flocks, including cancers such as ovine pulmonary adenocarcinoma (OPA) associated with exogenous Jaagsiekte sheep retrovirus (exJSRV) and nasal tumours associated with Enzootic Nasal Tumour Virus (ENTV) (Rosato et al., 2023). JSRV belongs to the

Retroviridae family, the Orthoretrovirinae subfamily, and the Beta retrovirus genus. Approximately twenty-seven endogenous retroviruses are also contained within the sheep genome. Known as endogenous Jaagsiekte sheep retroviruses (enJSRVs), these are closely related to JSRV and are transmitted vertically. In addition, exogenous JSRV has been shown to be particularly associated with pulmonary adenomatous tumours in sheep (Janardhan Yadav et al., 2024).

Ovine pulmonary adenocarcinoma (OPA), also referred to as ovine pulmonary adenomatosis or Jaagsiekte, manifests as a progressive, chronic, and highly contagious pulmonary disease primarily affecting small ruminants, mainly sheep (rarely goats and mouflons) (Quintas et al., 2021; Toma et al., 2025). OPA is frequently identified in regions such as South America, the United Kingdom, and South Africa, with consistent diagnoses reported across numerous European nations. Specifically, it is considered endemic in Scotland and Spain. The disease has not been found in Australia, Iceland, the Falkland Islands and New Zealand. Although rare, the disease has also been reported in sheep in North America (Quintas et al., 2021; Karakurt et al., 2022b; Ortega et al., 2023). The natural transmission of JSRV occurs via the aerogenous route, mainly by inhalation of cell-free particles, but oral transmission via transuterine or infected colostrum and milk may also contribute to disease development (Gray et al., 2019). Several studies have shown that JSRV infection can manifest in lambs during the perinatal period or within the initial months of their life. This condition has also been observed in adult sheep (Rosato et al., 2023). As there is no effective treatment or vaccine for the disease, it is difficult to control and eradicate it (Mansour et al., 2019; Özkan et al., 2020). The subclinical form of OPA affects growth rate, carcass weight, milk and wool production (Azizi et al., 2014). Due to the significant economic damage caused by OPA, the disease has been classified as a notifiable animal disease by the World Organisation for Animal Health (formerly the Office International des Epizooties) (Duan et al., 2024).

In addition to its importance in veterinary medicine, OPA constitutes a remarkable animal model for various forms of human lung adenocarcinomas (bronchial-alveolar cancer (BAC) or non-small cell lung cancer (NSCLC)) due to their shared histological characteristics and activation of oncogenic signalling pathways (Shadmehri *et al.*, 2022; Zhang *et al.*, 2024; Toma *et al.*, 2025). There are three forms of OPA: classical, atypical, and mixed (García-Goti *et al.*, 2000; Ortega *et al.*, 2023). OPA has been studied in our region, using molecular and pathological means indicating the presence of the virus (Coskun *et al.*, 2024). Unfortunately, present data is not enough to determine the prevalence of the disease considering the sample size of the studies.

The objective of this study was to determine the proliferation index via proliferating cell nuclear antigen (PCNA) expression, the p53 tumour suppressor gene status, and the angiogenesis status by carcinoembryogenic antigen (CEA) and vascular endothelial growth factor-A in both classical and atypical OPAs. This evaluation was conducted to ascertain whether notable distinctions exist in cancer behaviour between the different forms of OPA.

#### MATERIALS AND METHODS

Animals: The formalin-fixed, paraffin-embedded tissue samples used in this study were provided by the Department of Pathology, Faculty of Veterinary Medicine, Kafkas University, between 2022 and 2024. In the current study, 12 tumoral lung tissues of sheep with OPA, which were brought to the Department of Veterinary Pathology with severe respiratory complaints and systematically necropsied, were used as material. Of these 12 cases, six were in classical form and six were in atypical form.

Ethics committee report: The Animal Experiments Local Ethics Committee of Kafkas University approved the study (KAU-HADYEK-2025/035, Date: 04.03.2025).

**Nucleic acid extraction:** Sections were obtained from paraffin-embedded tissue blocks and placed into 1.5mL tubes for each case. The extraction of these samples was performed following the methodology outlined by Pikor *et al.* (2011), with a minor modification. Specifically, RNase was not added to maximize RNA yield.

Reverse transcription polymerase chain reaction (RT-PCR): Reverse transcription and polymerase chain reaction of the samples were conducted using 2X One-step RT-PCR kit from Hibrigen (Türkiye, Catalogue Number: MG-OSPM-01). The primer pair, as described by Mansour et al. (2019) were used. Reverse transcription was achieved by 40min at 55°C and PCR cycles were as follows: an initial denaturation step at 95°C for 5 minutes, followed by 35 cycles of denaturation at 95°C for 1 minute, annealing at 58°C for 1 minute, and extension at 72°C for 1 minute, with a final extension step at 72°C for 10 minutes (Coskun et al., 2024). The expected amplicon size was 398 base pairs.

Phylogenetic analysis: Positive amplicons (05 in total) were submitted for Sanger sequencing (BM Laboratuvar Sistemleri, Ankara). Sequence assembly and editing were conducted utilising Bioedit (Version 7.0.5.3) and Clustal W (Hall, 1999). Sequence similarities were assessed using the Basic Local Alignment Search Tool (BLAST) software from the National Center for Biotechnology Information (NCBI) (Altschul et al., 1997). Phylogenetic analysis was executed employing the neighbour-joining method in MEGA7 software (Tamura et al., 2011), evolutionary distances between sequences were computed using the Kimura two-parameter model (Karakurt et al., 2023b; Erkılıç et al., 2024). The confidence level of the NJ tree was evaluated through bootstrapping with 1000 replicates. Additionally, a comparative table of amino acid sequences was generated to identify variations. The similarity of the isolates was analyzed using the SDT software (Muhire et al., 2014).

Histopathological examinations: Sheep lung tissue samples underwent fixation in a 10% formaldehyde solution. Serial sections of 5-micron thickness were obtained from the paraffin blocks prepared after routine tissue follow-up procedures. The sections were then stained with haematoxylin and eosin (H&E) to assess tissue histopathological alterations. Detailed examination of the sections was conducted using a light microscope by at least two different pathologists. Noteworthy pathological findings were photographed at various magnifications (Karakurt *et al.*, 2023a).

Immunohistochemical examinations: Serial 4-micronthick sections of paraffin blocks of lung tissue were labelled with commercial antibodies for JSRV capsid protein (JSRV CA), PCNA, p53, CEA, and VEGF-A. The avidin-biotin-peroxidase technique was employed following the manufacturer's recommended protocols. Comprehensive details, including incubation times, clone numbers, and dilution ratios for the primary antibodies utilised, are shown in Table 1. The immunolabelling steps were performed in accordance with the instructions of the Thermo Scientific Histostain IHC Kit (HRP, broad-

spectrum, REF: TP-125-HL). Aminoethyl carbazole (AEC, Thermo Scientific, REF: TA-125-HA) and 3,3'diaminobenzidine (DAB, Thermo Scientific, REF: TA-125-HD) chromogens were used as chromogenic substrates, and the reaction was elicited by application for approximately 15 minutes. All sections were washed in tap water for 5 minutes and then exposed to Mayer's hematoxylin for approximately 1 minute. The sections treated with AEC chromogen were kept in distilled water and then covered with AEC mount. Sections treated with DAB chromogen were passed through low to high- graded alcohols and xylene, then covered with Entellan and examined under a light microscope (Olympus Bx53) and photographed using the Cell^P software (Olympus Soft Imaging Solutions GmbH, 3,4). The resulting photographs were subsequently analyzed in detail using ImageJ software (version 1.51j8).

Table I: Information on primary antibodies used in immunohistochemical examinations

initiations to the initial examinations									
Primary	Company and	CataloguePre-treatment	Dilution	Incubation					
Antibodies	Numbers			Conditions					
JSRV CA	Supplied by Pro	of. MassimoMicrowave	1/1500	Overnight,					
	Palmarini, poly	clonal oven		4°C					
PCNA	SantaCruz,	sc-56,Microwave	1/100	Overnight,					
	monoclonal	oven		4°C					
p53	ABclonal,	A0263, Microwave	1/100	Overnight,					
	polyclonal	oven		4°C					
CEA	ABclonal,	A12421, Microwave	1/100	Overnight,					
	polyclonal	oven		4 °C					
VEGF-A	ABclonal,	A5708, Microwave	1/100	Overnight,					
	polyclonal	oven		4 °C					

The immunohistochemical labelling results were analyzed using a grading system that was based on the quantification of positive cells within the areas where immunopositive reactions were examined and which most strongly reflected the labelling characteristic. To quantify immunopositive reactions in tissues, analysis commenced in areas displaying high-intensity reactions. For each case, three distinct regions of the tumour tissue were evaluated under a 40x objective. The number of positively labelled tumour cells and inflammatory cells in the tumour microenvironment was counted separately, and the mean number of positive cells for a given OPA case was calculated as the average of these 3 fields. Grading was recorded as (-) no immunoreactivity; (+) weak, 1-10% positivity; (++) moderate, 11-59% positivity and (++++) severe, over 60% positivity (Karakurt et al., 2022c).

**Statistical analysis:** The Mann-Whitney U test was employed in the comparison of classical and atypical OPA groups based on immunopositive cell scoring. Immunoreactivity scores for JSRV CA, PCNA, p53, CEA, and VEGF-A were reported as ± standard error of the mean (SEM). Statistical analyses were conducted using SPSS® (version 26.0, Chicago, IL, USA) with differences between the OPA groups considered significant if P <0.05 (Karakurt *et al.*, 2022a).

# **RESULTS**

Macroscopic findings: In sheep with classical OPA, white-greyish or pinkish areas of irregular and hard structure located in different lobes of the lungs were detected. These lungs were found to be poorly collapsed.

OPA lesions in the classical form were seen in the cranial, medial and caudal lobes. However, nodular or diffuse foci were much more common in the cranial lobes (cranioventral areas). In some regions, OPA lesions were seen to coalesce locally. In some cases, these lesions even covered a substantial part or the entire lobe. Tumour foci with a shiny or opaque appearance did not form a distinct bulge in the pleura. Lung weights were found to increase in direct proportion to the size of the tumour lesions and to increase in volume (many times more than normal). The tissue cross-sectional area of the tumour foci was found to be quite moist. In addition, the presence of foamy exudate in the bronchi and bronchioles was remarkable (Fig. 1a-b).

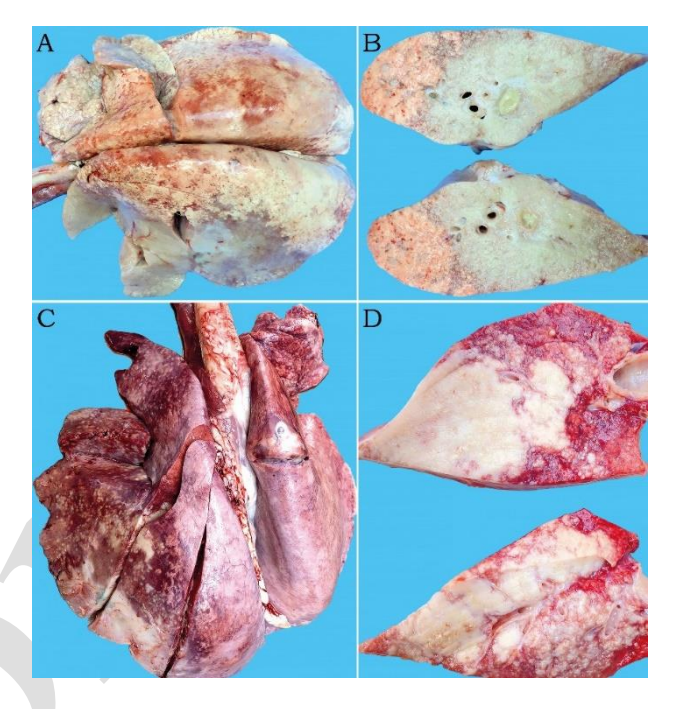


Fig. 1: Macroscopic and cross-sectional view of tumour tissue, A-B: Classical OPA and C-D: Atypical OPA

In the lungs of sheep with the atypical form of OPA, the lesions were mostly concentrated in the diaphragmatic lobes. The lesions were highly variable in size and well demarcated from the surrounding normal tissue. The consistency of these greyish solitary or multifocal nodular tumour foci was much harder and more solid than in the classical form. In addition, the cross-sectional surfaces of the atypical lesions were much drier than those of the classical form (Fig. 1c-d).

In light of these macroscopic findings, of 12 cases, 6 were diagnosed as classical OPA, and the remaining 6 were atypical OPA.

Molecular results: Among the 12 paraffin-embedded tissue samples, five tested positive via RT-PCR, exhibiting amplicons of the expected size at 398bp. The sequences of these amplicons were submitted to GenBank under accession numbers PV253894, PV253895, PV253896, PV253897, and PV253898. The construction of a phylogenetic tree was facilitated by the retrieval of reference sequences from GenBank (Fig. 2). Endogenous, type 1 and type 2 exogenous JSRV reference sequences were included in the alignment. To ensure a comprehensive analysis, other retroviruses were incorporated into the

study to serve as an outgroup. It was established that all of the study isolates were clustered with type 2 exJSRV references. The predicted amino acid content of the study isolates is illustrated in Fig. 3, based on their respective sequences. This revealed only minor variations in the 30 and 32<sup>nd</sup> positions, and only one amino acid was different at 63. Isolates exhibit a similarity range of 97.4-99.4% among themselves (Fig. 4).

**Histopathological findings:** The growth patterns of all OPA cases are shown in Table 2. In both classical (n=6)

and atypical (n=6) forms of OPA, tumour cells were found to be cubic or columnar. These tumour cells were observed to form acinar, papillary, or lepidic tumour structures in bronchioles or alveoli. In bronchioles and alveoli, sporadic finger-like processes extended into the lumen and masses of variable size were formed by tumour cells in the lumen. In some foci, acinar, papillary or lepidic growths were observed alone, whereas in most cases these three types of growth patterns accompanied each other. In addition, fibromyxoid growths were present in only one case. A very intense inflammatory cell infiltration was observed around

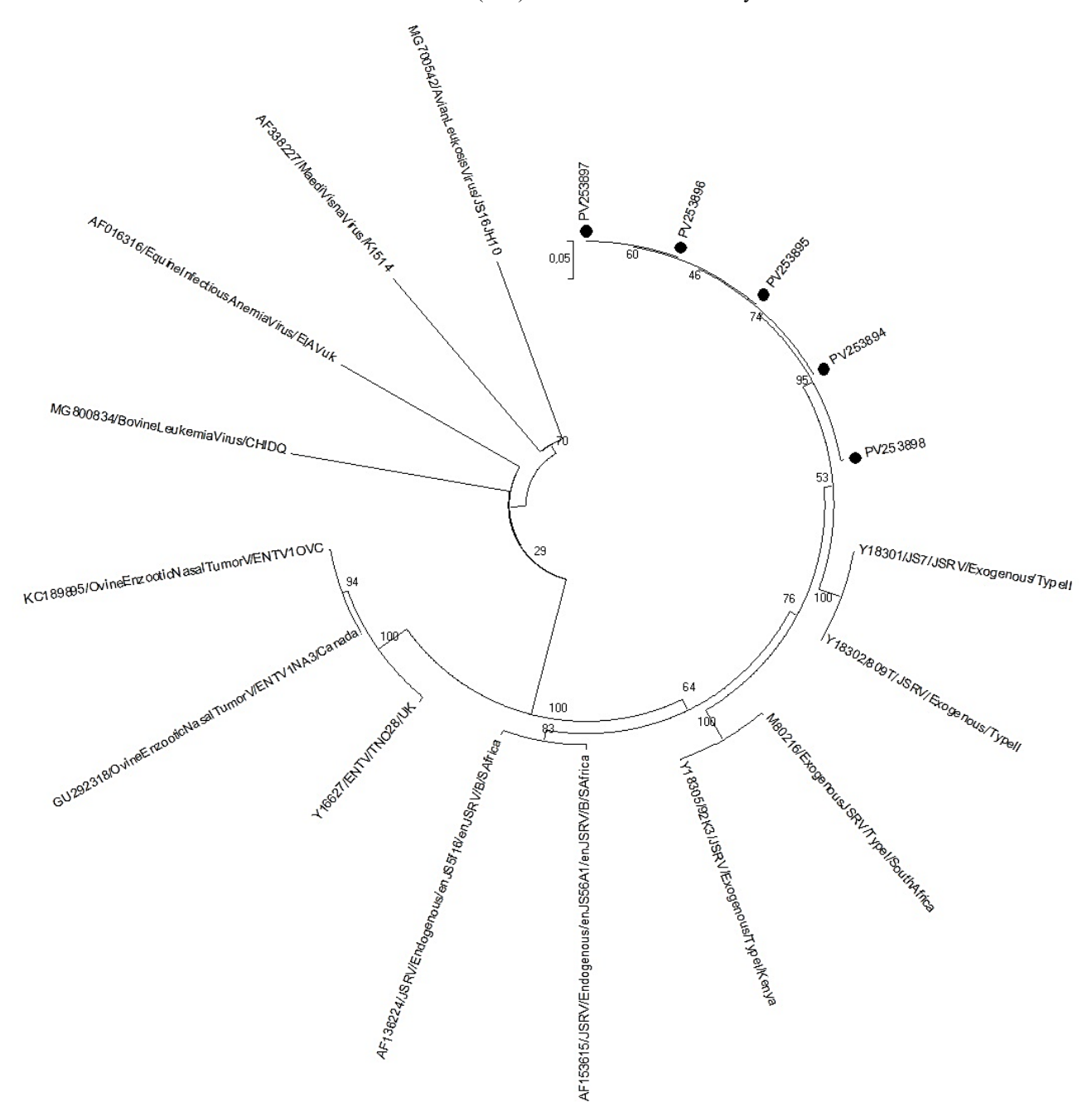


Fig. 2: Phylogenetic tree based on partial envelope gene. Study isolates are marked with black dots. Study isolates are clustered with exJSRV type 2 references.

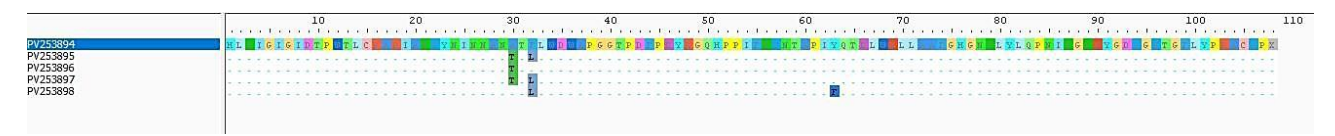


Fig. 3: Comparison of predicted amino acid sequences of the study. Differences are noted on 30, 32 and 63 positions.

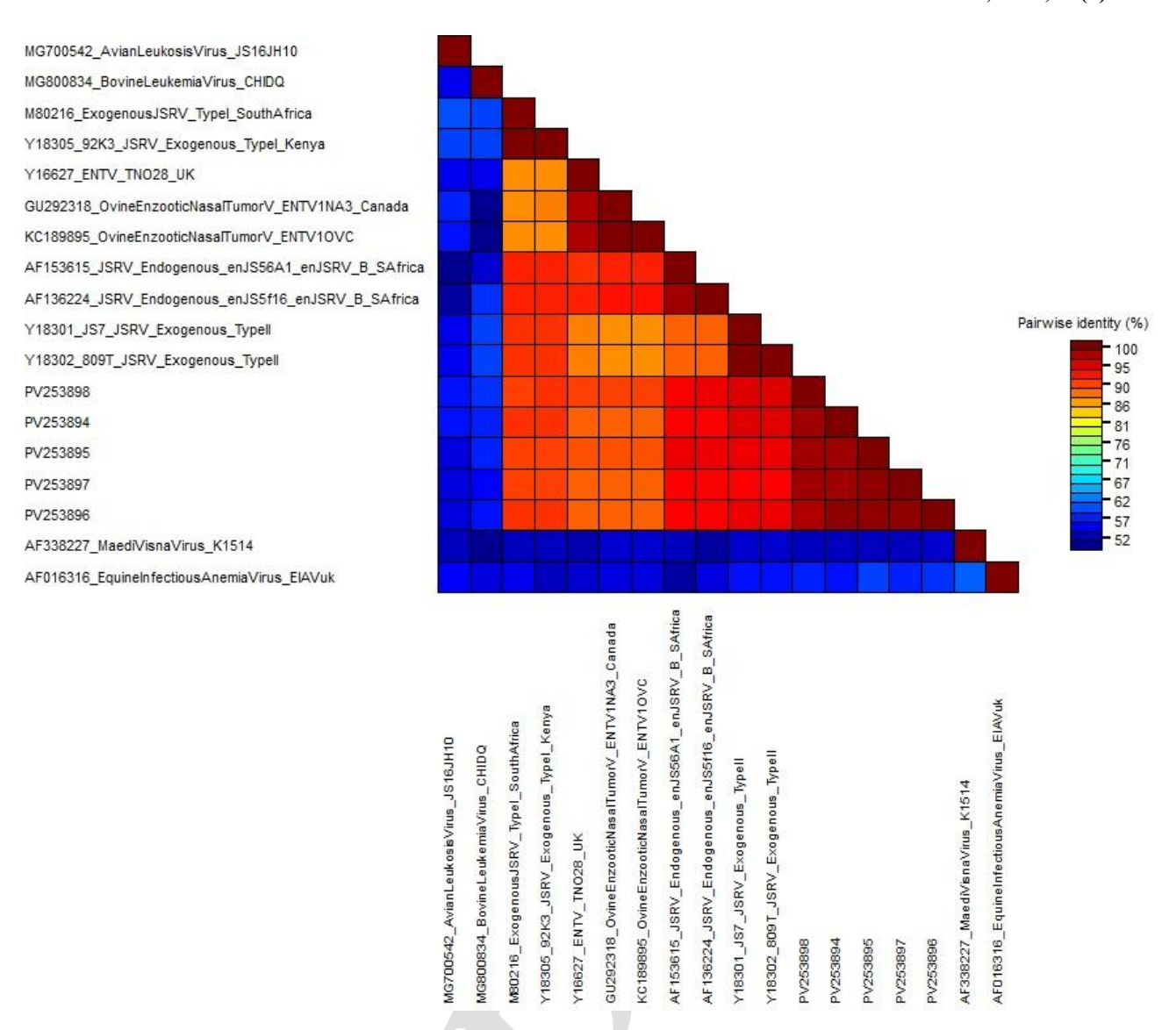


Fig. 4: Similarity of all references and study isolates. The graph is prepared using SDT software.

**Table 2:** Growth patterns and immunoreactivity scores of all OPAs

Case	Gross	Pattern	JSRV CA	PCNA	P53	CEA	VEGF-A
Ī	С	Papillary	+++	+++	++	+++	++
2	С	Papillary + Acinar	+++	+++	++	+++	+
3	С	Papillary + Acinar	+++	+++	++	++	+
4	С	Papillary	++	+++	+++	+++	++
5	C	Papillary	+++	+++	+++	+++	++
6	C	Lepidic + Fibromyxoid	++	++	++	+++	+++
7	Α	Papillary	++	++	+	++	+
8	Α	Papillary + Acinar	+++	++	+	++	+
9	Α	Acinar	++	+++	++	+++	+
10	Α	Papillary + Acinar	++	++	+	+++	++
11	Α	Acinar	++	+++	++	++	+
12	Α	Papillary + Acinar	+++	+++	++	++	++
Mean ± standard error values of Group C		$2.67 \pm 0.21^{a}$	$2.83 \pm 0.17^{a}$	$2.33 \pm 0.21^{a}$	$2.83 \pm 0.17^{a}$	$1.83 \pm 0.31^{a}$	
Classical (C) and Atypical (A) Group A		$2.33 \pm 0.21^{a}$	$2.50 \pm 0.22^{a}$	$1.50 \pm 0.22^{a}$	$2.33 \pm 0.21^{a}$	$1.33 \pm 0.21^{a}$	
OPA gro		P value < 0.05	0.394	0.394	0.065	0.180	0.310

C: Classical, A: Atypical

the tumour foci. The majority of inflammatory cells were alveolar macrophages. The cytoplasm of most alveolar macrophages in the tumour microenvironment was enlarged. Alveolar macrophage infiltration was much more severe in the atypical form than in the classical form. In addition to these cells, severe neutrophilic leukocyte infiltration was one of the notable histopathological findings in some cases. In fact, the extent of this cell infiltration was such that it masked the tumour structures in some areas.

Diffuse alveolar oedema was also present. Typical or atypical mitotic figures were almost absent. Tumour cells were mostly well differentiated, and pleomorphism was very low. The stroma around the alveoli and bronchioles exhibited a marked thickening due to increased mononuclear cells and connective tissue. In addition to these histopathological findings, bronchopneumonia, abscesses, large areas of necrosis, and verminous pneumonia were observed in some cases (Fig. 5a-d).

Immunohistochemical findings: Both classical and atypical OPA cases exhibited positive expression for JSRV CA, PCNA, p53, CEA, and VEGF-A. The immunoreactivity scores for all biomarkers are detailed in Table 2, and statistically significant differences in these markers between classical and atypical OPA groups are also shown at the end of the table. JSRV CA

immunoreactivity was observed in the cytoplasm of tumour cells arranged in papillary and acinar structures. No significant variation in JSRV CA expression was observed across acinar, papillary, and lepidic growth patterns. In addition, JSRV CA expression did not differ significantly between the classical and atypical groups (Fig. 6a-b). PCNA-positive reactions were predominantly located

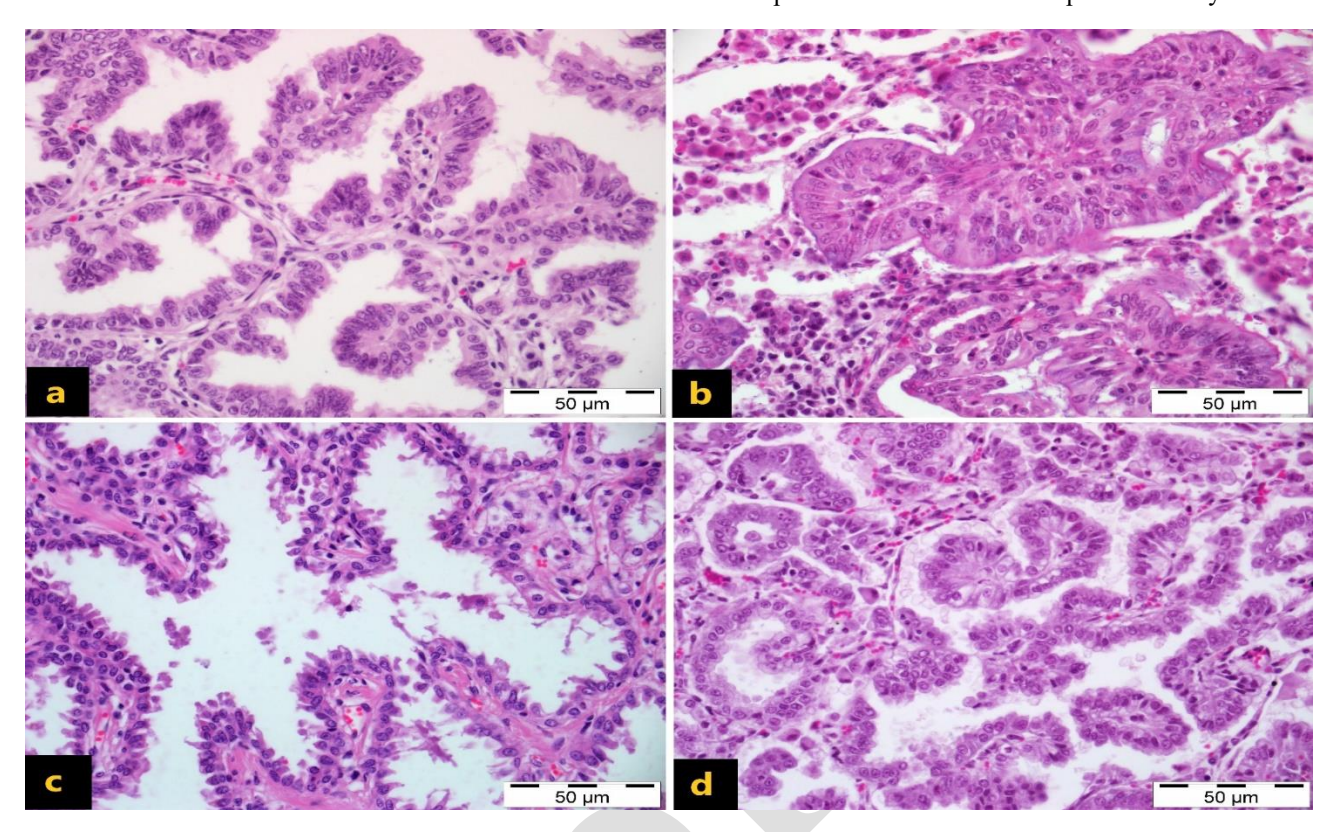


Fig. 5: OPA, H&E, a: Papillary pattern, finger-like projections extending into the lumen b: Acinar pattern, tubular structures formed by columnar neoplastic cells c: Lepidic pattern, palisaded cuboidal tumour cells lining the alveoli d: Mixed pattern (acinar and papillary structures).

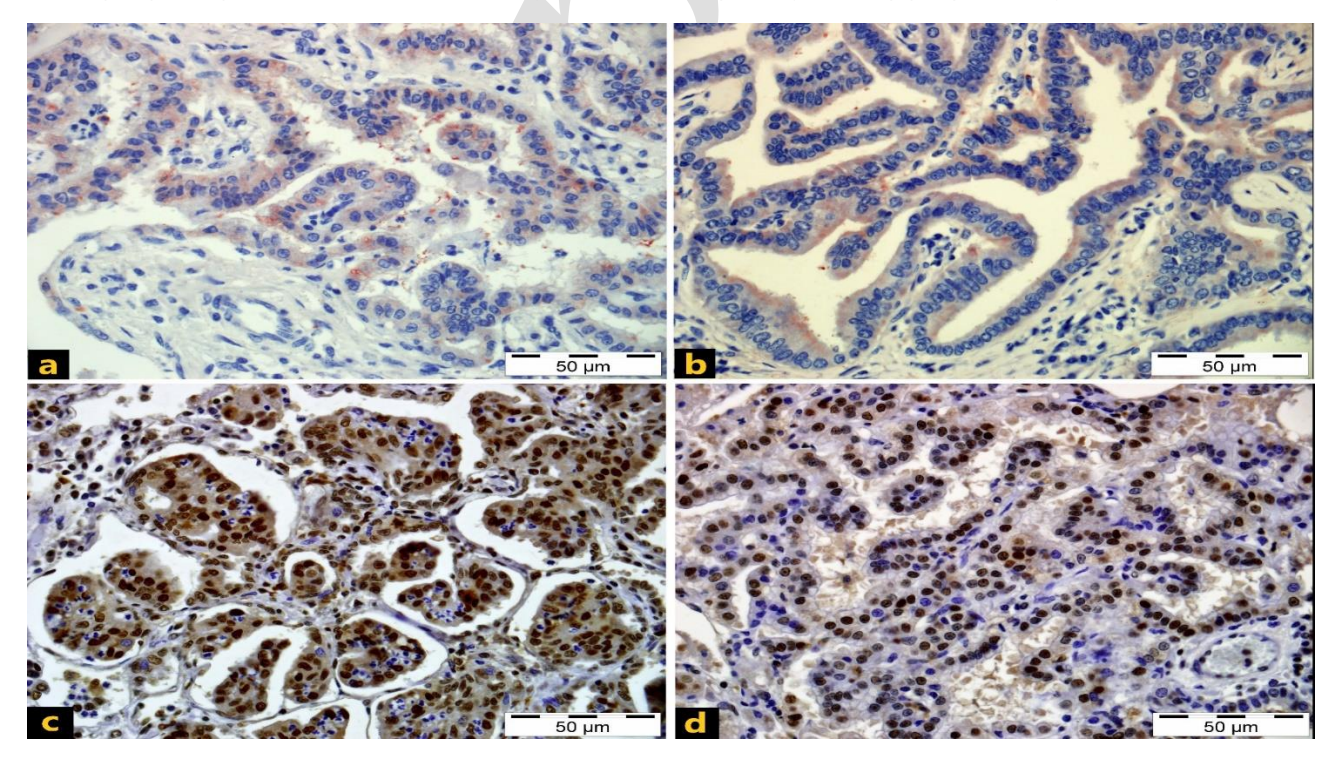


Fig. 6: a: Classical OPA, JSRV CA positive labelling in the cytoplasm of neoplastic cells b: Atypical OPA, membranous JSRV CA expression in tumour cells. JSRV CA, IHC, AEC. c: Classical OPA, nuclear PCNA immunopositive reactions in tumour cells forming papillary structures extending into the lumen. d: Atypical OPA, PCNA expression in the nuclei of neoplastic cells. PCNA, IHC, DAB.

within the nuclei of neoplastic cells, which constituted tubular structures within the alveoli and bronchioles, as well as finger-like extensions directed towards the lumen. However, positive labelling was also present locally in the stromal tissue. It was noted that PCNA immunoreactivity was much stronger in the papillary pattern than in the acinar pattern. It was also observed that PCNA expression was much higher in classical OPAs than in atypical OPAs. However, the difference between the two OPA groups was not significant (Fig. 6c-d). Similar to PCNA expression, p53 immunopositive reactions were detected in the nuclei of tumour cells in papillary and glandular structures extending into the lumen. In addition to nuclear labelling, p53 immunopositive reactions were also present in the cytoplasm of some cells. Compared to the acinar pattern, p53 protein expression was much stronger in the papillary pattern. However, there was no marked difference in p53 immunoreactivity between classical and atypical OPA

(Fig. 7a-b). CEA immunopositive labelling was dark brown and granular in the cytoplasm of tumour cells. CEA expression was observed not only in tumour cells but also in alveolar macrophages in the tumour microenvironment. CEA immunoreactivity was much more intense in the papillary pattern than in the acinar pattern. In addition, CEA expression was more pronounced in classical OPAs than in atypical OPAs. However, the observed difference between the two OPA groups did not reveal statistical significance (Fig. 7c-d). VEGF-A immunopositive labelling was intracytoplasmic and yellow-brownish in tumour cells. VEGF-A expression was very weak in both papillary and acinar patterns. The intensity of VEGF-A labelling in tumour cells exhibited no significant variation between the two patterns. Similarly, no statistically significant difference was observed in VEGF-A immunoreactivity among the different forms of OPA (Fig. 7e-f).

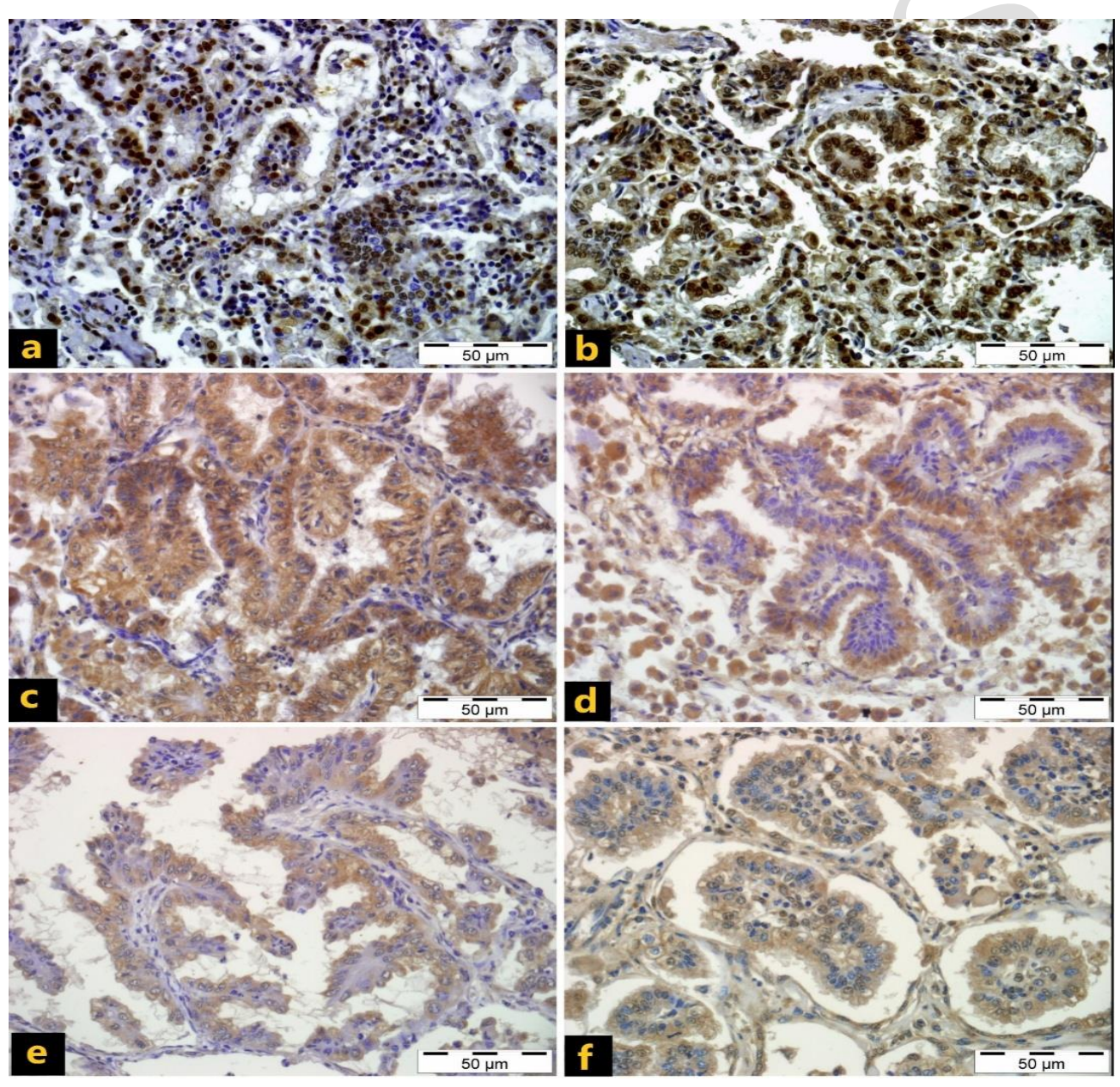


Fig. 7: a: Classical OPA, nuclear p53 positive labelling, b: Atypical OPA, p53 immunoreactivity in the nuclei of tumour cells. p53, IHC, DAB. c: Classical OPA, very strong intracytoplasmic CEA-positive labelling in tumour cells, d: Atypical OPA, CEA expression in the cytoplasm of tumour cells exhibiting papillary growths and in alveolar macrophages. CEA, IHC, DAB. e: Classical OPA, VEGF-A positive reactions in the cytoplasm of tumour cells forming finger-like processes. f: Atypical OPA, intracytoplasmic VEGF-A immunoreactivity in tumour cell masses in the alveolar lumen. VEGF-A, IHC, DAB.

#### DISCUSSION

The incubation period of OPA is long, with clinical manifestations potentially emerging years after ingestion of the viral agent (Azizi et al., 2014). Clinically, OPA is predominantly diagnosed in sheep (and, although rarely, in goats) aged 2-4 years (Scott et al., 2018). There is no species or sex predisposition to OPA (Toma et al., 2020). The main clinical signs of OPA are associated with cough. exercise intolerance, loss of appetite, reduced fitness, and emaciation (Rosato et al., 2023). If the tumour focus in the lung is small, the disease progresses subclinically (De Las Heras et al., 2021). An increase in lung tumour burden is associated with a concomitant rise in the production of surfactant-rich fluid by transformed epithelial cells, leading to substantial pulmonary effusions, nasal discharge, and progressive dyspnea, potentially exacerbated by physical exertion (Karagianni et al., 2019). In the advanced stages of the disease, up to 400mL of respiratory fluid can be discharged from the nostrils of the affected animal when the hindquarters of the affected animal are elevated (commonly known as the wheelbarrow test) (Youssef et al., 2015; Ortega et al., 2023). Deaths occur primarily due to secondary bacterial infections (Sonawane et al., 2016). The gold standard methods for diagnosing OPA are polymerase chain reaction (PCR), immunohistochemistry, postmortem and histopathological evaluation of suspected cancerous lung regions (Lee et al., 2017). In the current OPA was diagnosed using macroscopic, histopathological and immunohistochemical methods in lung tissue from 12 sheep with severe respiratory problems. However, molecular tests did not detect exJSRV nucleic acid in all tissues. Viral RNA was not identified in 7 out of the 12 tissues, a discrepancy potentially attributable to the limitations in utilizing paraffin-embedded tissue blocks. These 7 tissues could represent false negatives, given that histopathological and immunohistochemical analyses indicated the presence of OPA. Changes in the amino acids at positions 30 and 32 are observed, with only one amino acid exhibiting a different composition at position 63. This variation does not appear to hold significant importance. Macroscopically, OPA is classified into two forms: classical (diffuse) and atypical (nodular) (Hodor et al., 2024). The classical form is significantly more prevalent than the atypical form. However, the atypical form is less contagious (Toma et al., 2020). Although rare, intermediate or mixed forms have also been reported in various literature data (Ortega et al., 2023). In this study, 6 of the 12 cases were of the classical form and the other 6 were of the atypical form. There was no difference between the forms in terms of prevalence. In the classical presentation, the lungs fail to collapse and expand upon opening of the chest during necropsy. Neoplastic lesions may arise throughout the pulmonary tissue; however, they are more frequently observed in the cranio-ventral regions. These lesions exhibit a grey or purple hue, do not significantly protrude from the pleural surface, and demonstrate a firmer texture. Upon cross-sectional examination, the tumour lesions display a granular texture and a moist consistency, with a foamy fluid discharge from the bronchioles and bronchi upon the application of mild pressure (Quintas et al., 2021). In contrast to the classical form, the atypical form often presents as more nodular in

both early and advanced stages (De Las Heras et al., 2014). These nodules, which can be single or multiple and are most commonly located in the lobes of the diaphragm (Minguijón et al., 2013). Characterized by their pearly white colour and firm texture, these tumour lesions are sometimes clearly demarcated from the adjacent parenchymal tissue, exhibiting a dry surface (De Las Heras et al., 2021). In the current study, the tumour foci in classical OPAs tended to be localized mainly in the cranial lobes, whereas the involvement of the diaphragmatic lobes was more common in atvoical OPAs, which were well demarcated and displayed nodular growths. This is in line with the current literature (Minguijón et al., 2013; De Las Heras et al., 2014; De Las Heras et al., 2021; Quintas et al., 2021). However, the consistency of classical OPAs was much more moist, whereas atypical OPAs had a drier and firmer consistency.

JSRV is responsible for oncogenic transformation mainly in alveolar type II pneumocytes and, to a lesser extent, in Club cells (formerly Clara cells) (İlhan et al., 2016; Janardhan Yadav et al., 2024). Microscopic lesions are characterized by acinar or papillary growth of these cells. However, they are sometimes mixed with myxoid tissue. The current study noted that tumour cells exhibited papillary, acinar, lepidic, and mixed growth patterns. In some cases, only these patterns predominated, while in most cases, a mixed pattern of papillary and acinar growth was observed. However, lepidic and fibromyxoid growths were also present in a single case. The stroma consists of connective tissue fibrils, lymphocytes and plasma cells. In this study, the tumour-supporting tissue was markedly thickened by both connective tissue and mononuclear cell infiltration. The alveolar spaces around tumour foci are filled with macrophages and neutrophils (Minguijón et al., 2013). Within the study samples, in some cases neutrophil infiltration was so severe that some tumour foci were masked. In classical OPA, an inflammatory reaction consisting predominantly of neutrophils with proliferative changes, and adenomatosis is characteristic (Mishra et al., 2021). Microscopically, atypical OPA is characterized by proliferation deposition, fibroblast mononuclear cell infiltration (Griffiths et al., 2010; Summers et al., 2012). The growth pattern of tumour cells is acinar rather than papillary (Quintas et al., 2021). Contrary to this literature data, the mixed pattern was found to be much more prevalent than the acinar pattern in atypical OPA. In the classical presentation of OPA, the process of JSRV replication is predominantly attributable to the highly proliferative nature of the tumour, leading to enlargement of the tumour mass within the adjacent tissue, whereas in the atypical form, there is a reduced level of alveolar epithelial cell proliferation characterized by welldefined, non-progressive tumours (Mishra et al., 2021). In this study, no significant histopathological differences were observed between atypical and classical OPA forms. Only alveolar macrophages, which form the tumour microenvironment, were observed to significantly more in atypical OPA than in classical OPA.

OPA has been reported to metastasize to regional lymph nodes in 0.3-25% of cases (Minguijón *et al.*, 2013). However, metastases to distant tissues, such as the kidney, liver, heart, spleen, skeletal muscle, digestive system, skin, or adrenal glands, are very rare (Karakurt *et al.*, 2022d;

Ortega *et al.*, 2023). In the current study, no OPA-related metastatic lesions were found in regional lymph nodes or distant tissues and organs.

Proliferating cell nuclear antigen (PCNA) is a nonhistone nuclear protein that plays a role in the initiation of cell proliferation by enhancing the expression of DNA polymerase. The extent of PCNA expression is associated with tumour grade and mitotic activity (İlhan et al., 2016). PCNA expression has become a widely utilized method for the assessment of the proliferation rate of neoplastic pathologies, and at least 50% of cells in malignant tumours are usually PCNA-positive, and the number of PCNApositive cells is negatively correlated with prognosis. However, high PCNA expression is indicative of histological malignancy (Mishra et al., 2021). Mishra et al. (2021) found higher PCNA expression in classical OPAs compared to atypical OPAs and cases with bronchiolar hyperplasia. In the current study, PCNA expression was more intense in alveolar tumour cells forming finger-like projections that extended into the alveolar lumen, confirming the immunohistochemical findings of İlhan et al. (2016), Beytut et al. (2009), and Pawaiya and Kumar (2007). Tumour cells forming acinar structures were also positively labelled for PCNA expression. However, the intensity of labelling in these cells was milder than in alveolar tumour cells. Consistent with literature data (Mishra et al., 2021), PCNA immunopositive labelling was found to be much more intense in classical OPAs than in atypical OPAs. However, statistical analyses demonstrated that this difference between OPA forms was not significant. The immunohistochemical results of the study show that OPA has a very high proliferation index, regardless of growth pattern and form.

The p53 tumour suppressor gene has been demonstrated to be associated with the transcriptional activation of genes that are implicated in various cellular processes, including cell cycle regulation, DNA repair, genomic plasticity, senescence, angiogenesis and programmed cell death (Pawaiya and Kumar, 2007). Any damage or acquired mutations in the TP53 gene caused by many stress factors, such as DNA damage, hypoxia, viral infection and tumours, render the TP53 gene nonfunctional, leading to the escape of cancer cells from apoptosis and ultimately to carcinogenesis (İlhan et al., 2016; Mustafa et al., 2021). Neoplasms with mutations in the TP53 gene are much more aggressive, and the presence of a mutation in this gene in people with cancer significantly reduces patient survival (Shadmehri et al., 2022). The most significant genetic abnormalities observed in cases of lung cancer are mutations in the p53 gene and overexpression of the p53 protein (Ilhan et al., 2016). Shadmehri et al. (2022) used molecular methods to show that the TP53 gene was overexpressed in OPA-infected samples compared to healthy samples. They also reported a mutation in exon 4. In contrast to this study, Hudachek et al. (2010) found a p53 mutation in the DNA-binding domain (exons 5-8). Pawaiya and Kumar (2007) found that p53-positive labelling was intranuclear in papillary alveolar epithelial cells. In a similar study, Mustafa et al. (2021) reported, using immunohistochemical methods, that p53 expression was much more severe in advanced cases. However, they noted that p53-positive labelling was concentrated in the nuclei of tumour epithelial cells.

Conversely, İlhan et al. (2016) observed intracytoplasmic and intranuclear p53 reacted positively in tumour cells. In the current study, similar to this literature data (İlhan et al., 2016), intranuclear and intracytoplasmic p53 expressions were detected in neoplastic cells forming papillary and acinar structures. Furthermore, p53-positive labelling was much more intense in the papillary pattern than in the acinar pattern. However, no significant difference was found between OPA forms with regard to p53 immunoreactivity. The data from this study show that both classical and atypical OPA produce a positive reaction concerning the p53 tumour suppressor protein, especially in cases with a high proliferation index, where p53 immunoreactivity is much more severe. The severity of p53-positive reactions in the papillary pattern supports this conclusion.

CEA is an acidic glycoprotein that plays essential roles various functions such as intercellular adhesion, regulatory signal transmission, cell proliferation control, differentiation, apoptosis, angiogenesis, and immune response modulation (Lei et al., 2024). However, CEA is a reliable and highly useful tumour marker that can be used for cancer diagnosis, prognosis and treatment evaluation. Currently, serum CEA levels are widely used in the assessment of diagnosis, progression, recurrence and treatment of NSCLC, especially adenocarcinoma, and changes in serum CEA levels are closely associated with chemotherapy efficacy and prognosis (Gan et al., 2024). CEA is an important cancer marker not only for lung cancer, but also for gastrointestinal, genitourinary, pancreatic and breast cancer (Ghosh et al., 2013; Li et al., 2024). Although many studies have evaluated CEA levels in human medicine. particularly in lung cancer, there are only two references that have examined CEA levels specifically in OPA and enzootic nasal adenocarcinoma (ENA) (Ozmen et al., 2010; Özkan et al., 2020). Özkan et al. (2020) showed that CEA levels were elevated in OPA animals compared to healthy animals in the control group, but the difference between these two groups was not statistically significant. Ozmen et al. (2010) reported that the intensity of CEA labelling in tumour epithelial cells was very low in animals with ENA. In the current study, both classical and atypical OPAs showed positive responses in terms of CEA expression. However, there was no significant difference in CEA immunoreactivity between these different forms of OPA. CEA-positive labelling was mostly seen in tumour cells that formed finger-like processes. In the acinar pattern, the intensity of CEA labelling was weak. Similar to the findings of Özkan et al. (2020), the current study data show that CEA is not a very useful and reliable biomarker for OPA. We believe that the use of multiple biomarkers in combination with CEA will be much more effective in predicting the prognosis of the disease.

Angiogenesis, the process of forming new blood vessels from pre-existing vasculature, is a highly regulated mechanism. Cancer cells control the activation of angiogenesis through the release of various intercellular mediators. The vascular endothelial growth factor pathway, activated by the binding of VEGF to its receptors, represents the most critical signalling cascade in angiogenesis. Vascular endothelial growth factor (VEGF) is a homodimeric glycoprotein growth factor that binds to heparin and is specific to vascular endothelial cells. It significantly influences vasculogenesis, angiogenesis, endothelial cell

differentiation, inflammation, and tumour formation, as well as proliferation and migration (Serpin and Özmen, 2020). VEGFA, the first identified member of the VEGF family, exhibits expression across a spectrum of cell types, notably including cancer cells, and serves as a major inducer of angiogenesis, cancer cell proliferation, and migration. VEGFA promotes the expansion of the vascular network essential for tumour growth and metastasis and is frequently upregulated in cancers (Gomes et al., 2017). Serpin and Özmen (2020) reported increased VEGF immunoreactivity in sheep tumour cells with ENA. In contrast to this study. Gomes et al. (2017) found no VEGFA protein expression in JSRV-induced cancers, with very weak VEGFA expression in human lepidic adenocarcinomas. In the study by Sozmen and Beytut (2012), the expression of VEGF-C in OPAs was examined by immunohistochemistry, and it was reported that only a few cases were labelled positively for VEGF-C expression. In the current study, intracytoplasmic VEGF-A positive labelling, although very weak, was found in the cytoplasm of both acinar, papillary and lepidic/fibromyxoid tumour cells in atypical and classical OPAs. In this study, no local or distant tissue metastases were detected in any of the 12 OPA cases. It was interpreted that low VEGF-A expression may be related to the low metastatic and malignant potential of OPAs.

Conclusions: Immunohistochemical data from the current study showed that different forms of OPAs have a very high proliferation index, regardless of their growth pattern. It also showed that the p53 tumour suppressor gene is involved in the pathogenesis of OPAs, similar to human lung cancer. The assessment of CEA expression alone was found to be potentially a controversial and misleading biomarker in the diagnosis and progression of OPA. Although OPAs showed a high proliferation index, the low metastatic potential of OPAs was also supported by low VEGF-A expression. However, when macroscopic (classical or atypical) and molecular data (all isolates were type 2 with minor amino acid changes) do not seem to have great importance in the overall disease onset.

**Author's Contribution:** EK and NC concept, idea, writing, AYU and SG histopathology and immunohistochemistry, EK and EB histopathological and immunohistochemical analyses, ÖFK, TY and HAÇ systematic necropsy

**Financial Support**: The authors declare that this study has received no financial support.

**Acknowledgements:** We would like to express our gratitude to Professor Massimo Palmarini (Institute of Comparative Medicine, Faculty of Veterinary Medicine, University of Glasgow, UK) for providing the rabbit anti-JSRV CA primary antibody.

**Conflict of Interest:** The authors declared that there is no conflict of interest.

#### REFERENCES

Altschul SF, Madden TL, Schäffer AA, et al., 1997. Gapped BLAST and PSI-BLAST: a new generation of protein database search programs. Nucleic Acids Res 25:3389–3402.

- Azizi S, Tajbakhsh E and Fathi F, 2014. Ovine pulmonary adenocarcinoma in slaughtered sheep: a pathological and polymerase chain reaction study. | S Afr Vet Assoc 85:932.
- Beytut E, Sözmen M and Ergínsoy S, 2009. Immunohistochemical detection of pulmonary surfactant proteins and retroviral antigens in the lungs of sheep with pulmonary adenomatosis. | Comp Pathol 140:43–53.
- Coskun N, Yilmaz V, Karakurt E, et al., 2024. Molecular and pathological detection of Jaagsiekte sheep retrovirus in lung tissues of sheep. Kafkas Univ Vet Fak Derg 30:809-14.
- De Las Heras M, Borobia M and Ortín A, 2021. Neoplasia-associated wasting diseases with economic relevance in the sheep industry. Animals (Basel) 11:381.
- De Las Heras M, de Martino A, Borobia M, et al., 2014. Solitary tumours associated with Jaagsiekte retrovirus in sheep are heterogeneous and contain cells expressing markers identifying progenitor cells in lung repair. I Comp Pathol 150:138–47
- Duan X, Shi X, Zhang P, et al., 2024. Identification of concurrent infection with Jaagsiekte sheep retrovirus and maedi-visna virus in China. J Vet Sci 25:e61.
- Erkılıç EE, Coşkun N, Kırmızıgül AH, et al., 2024. Molecular investigation of viral agents in cattle with respiratory system problems. Kafkas Univ Vet Fak Derg 30:707-12.
- Gan T, An W, Long Y, et al., 2024. Correlation between carcinoembryonic antigen (CEA) expression and EGFR mutations in non-small-cell lung cancer: a meta-analysis. Clin Transl Oncol 26:991–1000.
- García-Goti M, González L, Cousens C, et al., 2000. Sheep pulmonary adenomatosis: characterization of two pathological forms associated with jaagsiekte retrovirus. J Comp Pathol 122:55–65.
- Ghosh I, Bhattacharjee D, Das AK, et al., 2013. Diagnostic role of tumour markers CEA, CA15-3, CA19-9 and CA125 in lung cancer. Indian J Clin Biochem 28:24–29.
- Gomes M, Archer F, Girard N, et al., 2017. Blocked expression of key genes of the angiogenic pathway in JSRV-induced pulmonary adenocarcinomas. Vet Res 48:76.
- Gray ME, Meehan J, Sullivan P, et al., 2019. Ovine pulmonary adenocarcinoma: a unique model to improve lung cancer research. Front Oncol 9:335.
- Griffiths DJ, Martineau HM, Cousens C, 2010. Pathology and pathogenesis of ovine pulmonary adenocarcinoma. J Comp Pathol 142:260–283.
- Hall TA, 1999. BioEdit: A user-friendly biological sequence 457 align-ment editör and analysis program for Windows 95/98/NT. Nucleic Acids Symp Ser 41:95-98.
- Hodor D, Toma C, Negoescu A, et al., 2024. Retroviral coinfection (Jaagsiekte and Maedi-Visna viruses) in sheep with pulmonary tumors in Transylvania (Romania): retrospective study on 82 cases. Front Vet Sci 11: 1457971.
- Hudachek SF, Kraft SL, Thamm DH, et al., 2010. Lung tumor development and spontaneous regression in lambs coinfected with Jaagsiekte sheep retrovirus and ovine lentivirus. Vet Pathol 47:148–162.
- Ilhan F, Vural SA, Yıldırım S, et al., 2016. Expression of p53 protein, Jaagsiekte sheep retrovirus matrix protein, and surfactant protein in the lungs of sheep with pulmonary adenomatosis. J Vet Diagn Invest 28:249–256.
- Janardhan Yadav E, Prabhakar YK, Shanmugam G, et al., 2024. Whole genome characterization of jaagsiekte sheep retrovirus isolated from OPA infected sheep (India) and structural assessment (Insilico) of proteins of JSRV. The Microbe 3:100068
- Karagianni AE, Vasoya D, Finlayson J, et al., 2019. Transcriptional response of ovine lung to infection with jaagsiekte sheep retrovirus. J Virol 93:e00876-19.
- Karakurt E, Beytut E, Dağ S, et al., 2022a. Assessment of MDA and 8-OHdG expressions in ovine pulmonary adenocarcinomas by immunohistochemical and immunofluorescence methods. Acta Vet Brno 91:235–41.
- Karakurt E, Beytut E, Dağ S, et al., 2022b. Immunohistochemical detection of pro-inflammatory and anti-inflammatory interleukins in the lungs of sheep with jaagsiekte. Turkish J Vet Res 6:9-14.
- Karakurt E, Beytut E, Dağ S, et al., 2022c. Immunohistochemical detection of TNF- $\alpha$  and IFN- $\gamma$  expressions in the lungs of sheep with pulmonary adenocarcinomas. Acta Vet Eurasia 48:161-66.
- Karakurt E, Beytut E, Dağ S, et al., 2022d. The relationship between metastasis and MMP-9 in sheep with pulmonary adenocarcinomas. Kafkas Univ Vet Fak Derg 28:211-16.
- Karakurt E, Coşkun N, Beytut E, et al., 2023a. Evaluation of the relationship between inflammatory reaction and interleukins in ovine pulmonary adenocarcinomas. Vet Res Forum 14:1–6.

- Karakurt E, Coşkun N, Beytut E, et al., 2023b. Immunohistochemical assessment of MDA and 8-OHdG expression in the skin, lungs and kidneys of lambs naturally infected with sheeppox virus confirmed with PCR. Kafkas Univ Vet Fak Derg 29:483-90.
- Lee AM, Wolfe A, Cassidy JP, et al., 2017. First confirmation by PCR of Jaagsiekte sheep retrovirus in Ireland and prevalence of ovine pulmonary adenocarcinoma in adult sheep at slaughter. Ir Vet J 70:33.
- Lei J, Wu L, Zhang N, et al., 2024. Carcinoembryonic antigen potentiates non-small cell lung cancer progression via PKA503 PGC-1α axis. Mol Biomed 5:19.
- Li L, Xu Y, Wang Y, et al., 2024. The diagnostic and prognostic value of the combination of tumor M2-pyruvate kinase, carcinoembryonic antigen, and cytokeratin 19 fragment in non-small cell lung cancer. Technol Cancer Res Treat 23:15330338241265983.
- Mansour KA, Al-Husseiny SH, Kshash QH, et al., 2019. Clinical-histopathological and molecular study of ovine pulmonary adenocarcinoma in Awassi sheep in Al-Qadisiyah Province, Iraq Vet World 12:454–58.
- Minguijón E, González L, De las Heras M, et al., 2013. Pathological and aetiological studies in sheep exhibiting extrathoracic metastasis of ovine pulmonary adenocarcinoma (Jaagsiekte). J Comp Pathol 148:139–47.
- Mishra S, Kumar P, Dar JA, et al., 2021. Differential immunohistochemical expression of JSRV capsid antigen and tumour biomarkers in classical and atypical OPA: a comparative study. Biol Rhythm Res 52:946–56.
- Muhire BM, Varsani A and Martin DP, 2014. SDT: a virus classification tool based on pairwise sequence alignment and identity calculation. PloS One 9:e108277.
- Mustafa ES, Al-Jameel WH and Al-Mahmood SS, 2021. Immunohistochemical detection of P53 and Mdm2 and its correlation with histological grading system in ovine pulmonary adenocarcinoma. Iraqi J Vet Sci 35:687-92.
- Ortega J, Corpa JM, Castillo D, et al., 2023. Pathological spectrum of ovine pulmonary adenocarcinoma in small ruminants: a focus on the mixed form. Animals (Basel) 13:2828.
- Ozmen O, Sahinduran S, Haligur M, et al., 2010. Clinical, pathological, immunohistochemical and ultrastructural observations on enzootic nasal adenocarcinoma in five goats. Kafkas Univ Vet Fak Derg 16:633-39.
- Özkan C, Yıldırım S, Huyut Z, et al., 2020. Selected tumour biomarker levels in sheep with pulmonary adenomatosis. J Vet Res 64:39–44.
- Pawaiya RVS and Kumar R, 2007. Ovine pulmonary adenocarcinoma: evaluation of molecular tumour markers. Indian J Vet Pathol 31:99-107.

- Pikor LA, Enfield KS, Cameron H, et al., 2011. DNA extraction from paraffin embedded material for genetic and epigenetic analyses. J Vis Exp 49:2763.
- Quintas H, Pires I, Garcês A, et al., 2021. The diagnostic challenges of ovine pulmonary adenocarcinoma. Ruminants 1:58-71.
- Rosato G, Abril C, Hilbe M, et al., 2023. A combined approach for detection of ovine small ruminant retrovirus co-infections. Viruses 15:376.
- Scott PR, Dagleish MP and Cousens C, 2018. Development of superficial lung lesions monitored on farm by serial ultrasonographic examination in sheep with lesions confirmed as ovine pulmonary adenocarcinoma at necropsy. Ir Vet J 71:23.
- Serpin N and Özmen Ö, 2020. Vascular endothelial growth factor and epithelial cell adhesion molecule immunoexpression in enzootic nasal adenocarcinoma of goats. Ankara Üniv Vet Fak Derg 67:51-57.
- Shadmehri M, Ashrafi-Helan J and Firouzamandi M, 2022. Mutation and up-regulation of TP53 in ovine pulmonary adenocarcinoma lung cells as a model of human lung cancer. Vet Res Forum 13:349–56.
- Sonawane GG, Tripathi BN, Kumar R, et al., 2016. Diagnosis and prevalence of ovine pulmonary adenocarcinoma in lung tissues of naturally infected farm sheep. Vet World 9:365–70.
- Sozmen M and Beytut E, 2012. An investigation of growth factors and lactoferrin in naturally occurring ovine pulmonary adenomatosis. J Comp Pathol 147:441–51.
- Summers C, Benito A, Ortin A, et al., 2012. The distribution of immune cells in the lungs of classical and atypical ovine pulmonary adenocarcinoma. Vet Immunol Immunopathol 146:1–7.
- Tamura K, Peterson D, Peterson N, et al., 2011. MEGA5: molecular evolutionary genetics analysis using maximum likelihood, evolutionary distance, and maximum parsimony methods. Mol Biol Evol 28:2731–39.
- Toma C, Bâlteanu VA, Tripon S, et al., 2020. Exogenous jaagsiekte sheep retrovirus type 2 (exJSRV2) related to ovine pulmonary adenocarcinoma (OPA) in Romania: prevalence, anatomical forms, pathological description, immunophenotyping and virus identification. BMC Vet Res 16:296.
- Toma C, Popa R, Ciobanu L, et al., 2025. Overexpression of IL-6 and STAT3 may provide new insights into ovine pulmonary adenocarcinoma development. BMC Vet Res 21:29.
- Youssef G, Wallace WA, Dagleish MP, et al., 2015. Ovine pulmonary adenocarcinoma: a large animal model for human lung cancer. ILAR | 56:99–115.
- Zhang L, Yang H, Duan X, et al., 2024. Modulation of autophagy affected tumorigenesis induced by the envelope glycoprotein of JSRV. Virology 594:110059.